Microbial ecosystem dynamics drive fluctuating nitrogen loss in marine anoxic zones

Justin L. Penn[a,1], Thomas Weber[b], Bonnie X. Chang[c,d], and Curtis Deutsch[a,e]

[a]School of Oceanography, University of Washington, Seattle, WA 98195; [b]Department of Earth and Environmental Sciences, University of Rochester, Rochester, NY 14627; [c]Joint Institute for the Study of the Atmosphere and Ocean, University of Washington, Seattle, WA 98195; [d]Pacific Marine Environment Laboratory, National Oceanic and Atmospheric Administration (NOAA), Seattle, WA 98115; and [e]Department of Biology, University of Washington, Seattle, WA 98195

Edited by Donald E. Canfield, Institute of Biology and Nordic Center for Earth Evolution, University of Southern Denmark, Odense M, Denmark, and approved February 27, 2019 (received for review October 19, 2018)

The dynamics of nitrogen (N) loss in the ocean's oxygen-deficient zones (ODZs) are thought to be driven by climate impacts on ocean circulation and biological productivity. Here we analyze a data-constrained model of the microbial ecosystem in an ODZ and find that species interactions drive fluctuations in local- and regional-scale rates of N loss, even in the absence of climate variability. By consuming O_2 to nanomolar levels, aerobic nitrifying microbes cede their competitive advantage for scarce forms of N to anaerobic denitrifying bacteria. Because anaerobes cannot sustain their own low-O_2 niche, the physical O_2 supply restores competitive advantage to aerobic populations, resetting the cycle. The resulting ecosystem oscillations induce a unique geochemical signature within the ODZ—short-lived spikes of ammonium that are found in measured profiles. The microbial ecosystem dynamics also give rise to variable ratios of anammox to heterotrophic denitrification, providing a mechanism for the unexplained variability of these pathways observed in the ocean.

microbial ecology | oxygen minimum zones | nitrogen cycle | species oscillations

Bioavailable nitrogen (N) is a key macronutrient that limits the rates of biological activity. In the ocean, the concentration of nitrate (NO_3^-), the major form of bioavailable N, is reduced by anaerobic reduction to biologically inert N_2 gas within small subsurface O_2-deficient zones (ODZs) (1). The volumetric rate of N removal within these zones is limited by the downward flux of organic matter from sinking particles (2). In turn, ODZ volumes are strongly dependent on the regional O_2 content of the thermocline in which they reside (3). Variations in climate have major impacts on the supply of O_2 and organic matter to the ODZ, driving changes in the magnitude of N removal across a wide spectrum of timescales, from months to millennia (4–6).

Microbial community structure also plays a major role in regulating N_2 gas production. Anaerobic processes, such as anammox and heterotrophic denitrification, can tolerate up to micromolar amounts of O_2, allowing them to coexist with aerobic nitrifying microbes, which become limited by O_2 only at nanomolar concentrations (2, 7–14). Because both anaerobic and aerobic metabolisms utilize the key N-cycle intermediates ammonium (NH_4^+) and nitrite (NO_2^-) as substrates, their coexistence results in resource competition whose outcome is determined by nanomolar variations in O_2 (15). When nitrification is dominant, the reoxidation of partially denitrified NO_2^- to nitrate (NO_3^-) reduces the magnitude of N_2 production and increases O_2 consumption; when aerobic nitrifiers are excluded by O_2 scarcity, NO_3^- is efficiently reduced all of the way to N_2 (15, 16). Here we demonstrate that resource competition between aerobic nitrifiers, anaerobic denitrifiers, and anammox bacteria can also lead to regional-scale temporal variability in the rates of N and O_2 cycling, even with constant physical fluxes of O_2 and organic matter into the ODZs.

To examine the role of microbial interactions in the dynamics of fixed N loss, we analyzed a microbial ecosystem model (15) embedded within an ocean general circulation model (17, 18). The steady three-dimensional ocean circulation is optimized to fit tracer observations (temperature, salinity, radiocarbon, and CFC-11), implying realistic ventilation rates and pathways of the ODZs (19). We focus on the world's largest ODZ, in the eastern tropical North Pacific (ETNP) (20), by restricting the boundaries of the model from the equator to 35° N, the coast to 180° W, and the surface ocean to 2,000-m depth. Observed annual mean concentrations of O_2 and NO_3^- (21) are transported into the domain at its open boundaries to ensure their realistic supply to the ODZ region. The circulation does not vary over time, leaving microbial ecosystem dynamics as the sole source of temporal variability.

The microbial ecosystem model simulates the biomass of four microbial functional groups and the biogeochemical cycles of N and O_2 (15). In the surface ocean, phytoplankton produce dissolved organic nitrogen (DON) and sinking organic particles from inorganic N (NH_4^+, NO_2^-, NO_3^-). DON is remineralized by heterotrophic bacteria using O_2, or multistep denitrification (reduction of NO_3^- to NO_2^-, then to N_2) below a critical O_2 threshold (O_2^{crit}). The NH_4^+ and NO_2^- released by heterotrophs is used by autotrophs: slow growing and O_2-inhibited anammox bacteria, or aerobic archaea and bacteria that either perform NH_4^+ or NO_2^- oxidation with nanomolar O_2 sensitivities. Autotrophs assimilate NH_4^+ from seawater for growth. Because the

Significance

The removal of bioavailable nitrogen (N), a critical nutrient that limits marine primary production, is thought to vary due to climate forcing of the ocean's low oxygen zones. Here we demonstrate that competition between aerobic and anaerobic microbes for scarce resources drives fluctuations in the rate of marine N loss over time, even in a stable environment. Biological oscillations have been theorized for nearly a century in idealized models, but are shown here for the first time in a three-dimensional and data-constrained model of ocean circulation. A predicted geochemical signature of the oscillations is detected in environmental samples. This previously overlooked source of natural variability reconciles conflicting empirical evidence for the dominance of heterotrophic versus autotrophic pathways of N removal.

Author contributions: J.L.P. and C.D. designed research; J.L.P. performed research; J.L.P., T.W., and C.D. analyzed model output; B.X.C. made $NH4^+$ measurements; J.L.P. and C.D. wrote the paper; and T.W. and B.X.C. provided input on the paper.

The authors declare no conflict of interest.

This article is a PNAS Direct Submission.

Data deposition: Data related to this work have been deposited in Figshare.com; doi: 10.6084/m9.figshare.7627439.

[1]To whom correspondence should be addressed. Email: jpenn@uw.edu.

This article contains supporting information online at www.pnas.org/lookup/suppl/doi:10.1073/pnas.1818014116/-/DCSupplemental.

Published online March 25, 2019.

C:N ratio of bacterial biomass (6.8 ± 1.2) (22) matches that of organic matter within the ODZ (6.8) (2) heterotrophs satisfy their nutrient demand via NH_4^+ remineralized from DON (23). DON is released by phytoplankton, sinking particles, and all microbial populations during mortality.

In previous work (15), we assessed the model fit to observed long-term mean (climatological) fields of O_2 and NO_3^-, and profile compilations of NH_4^+, NO_2^-, and biologically produced N_2 gas (N_2^{xs}) from within the ETNP. These data reflect the characteristic vertical profiles of key chemical indicators of the metabolic status of the ODZs: subsurface maxima in NO_2^- and N_2^{xs}, reduced accumulations of NO_3^-, and nanomolar levels of NH_4^+ and O_2 (*SI Appendix*, Fig. S1). To constrain uncertainty in model parameters, we varied microbial growth, mortality, and nutrient affinities over two orders of magnitude, spanning values observed in laboratory cultures and process studies (*SI Appendix*, Table S1), and compared the resulting simulated profiles to the observations (*SI Appendix*, Fig. S1). Of the 90 parameter combinations tested, half reproduce all observed chemical profiles simultaneously, implying a realistic balance of physical and biological fluxes of N and O_2. This ensemble of model simulations that reproduce the data are used for further analysis and to quantify the sensitivity of our main results.

The simulated rate of regional N loss aligns with geochemical estimates based on measurements of the accumulation of N_2^{xs}, the deficits of NO_3^-, and its isotopes (19, 24), but fluctuates strongly over time (Fig. 1*A*) despite the steady rates of ocean circulation. These fluctuations are not caused by changes in the flux of organic matter or the physical supply of O_2 to the ODZ region, which are stable (*SI Appendix*, Fig. S2). The fluctuations persist across a wide range of physiological and ecological assumptions: regardless of the precise O_2 sensitivities of the microbial populations (yellow, red, and green lines in Fig. 1*A*); with and without inclusion of dissimilatory NO_3^- reduction to NH_4^+ (DNRA) (25) (blue line in Fig. 1*A*); whether heterotrophic denitrification is represented as a facultative or obligate process (1, 26) or if its steps are mediated by a single or multiple populations (27) (*SI Appendix*, Fig. S3). Fluctuations in N loss are found under all ecosystem model parameter combinations that satisfy the available tracer data constraints (*SI Appendix*, Fig. S4). Their amplitude is large relative to time-mean rates, averaging 43% ± 35% (SD) on regional scales and 233% ± 123% (SD) at the locations where fluctuations occur. While the regionally integrated N-loss rate lacks a characteristic frequency, local rates of N loss vary through semiregular oscillations (Fig. 1*B*). The complex fluctuations in the regional-scale N loss (Fig. 1*A*) thus arise from the integration of the many localized oscillators with distinct periods, phasing, and amplitudes.

The oscillations are also evident in aerobic metabolic rates, which together with the changes in N loss, drive large-scale fluctuations in the concentrations of O_2, NH_4^+, and NO_2^-, (Fig. 2). Fluctuations are strongest at the edge of the ODZ's anoxic core, in a "suboxic" zone, where the full diversity of simulated microbial populations coexist—aerobic NH_4^+ and NO_2^- oxidizers as well as autotrophic anammox bacteria and heterotrophic denitrifiers (15). In the anoxic core of the ODZ, where aerobic metabolisms are excluded, the chemical environment, the resident microbial populations, and their metabolic rates are relatively stable over time. The coincidence of variability in zones of long-term nitrifier–denitrifier coexistence implies that the oscillations are driven by interactions between these microbial groups. Indeed, if the nitrifiers are separated from autotrophic anammox and heterotrophic denitrifiers by imposing nonoverlapping O_2 thresholds, oscillations do not arise in the model simulations (*SI Appendix*, Fig. S5).

The mechanism of these oscillations derives from a fundamental ecosystem dynamic: consumption of O_2 by aerobic microbes provides an advantage for anaerobes, but their niche cannot be sustained against the physical O_2 supply without intermittent dominance of the aerobes. In the model ODZ, the consumption of O_2 by NO_2^- oxidation (~41 Tg O_2 y^{-1}) vastly outweighs NH_4^+oxidation (~4.9 Tg O_2 y^{-1}); NH_4^+oxidation thus plays little role in the oscillatory dynamic. The complete ecological sequence of the oscillation is illustrated by the phase diagram of NH_4^+ and O_2 at a single point in space (Fig. 3). When O_2, NH_4^+, and NO_2^- are plentiful, NO_2^- oxidizing bacteria experience net population growth (location Fig. 3 *A* and *B*, *i*). Their metabolic rate exceeds the physical O_2 supply and depletes

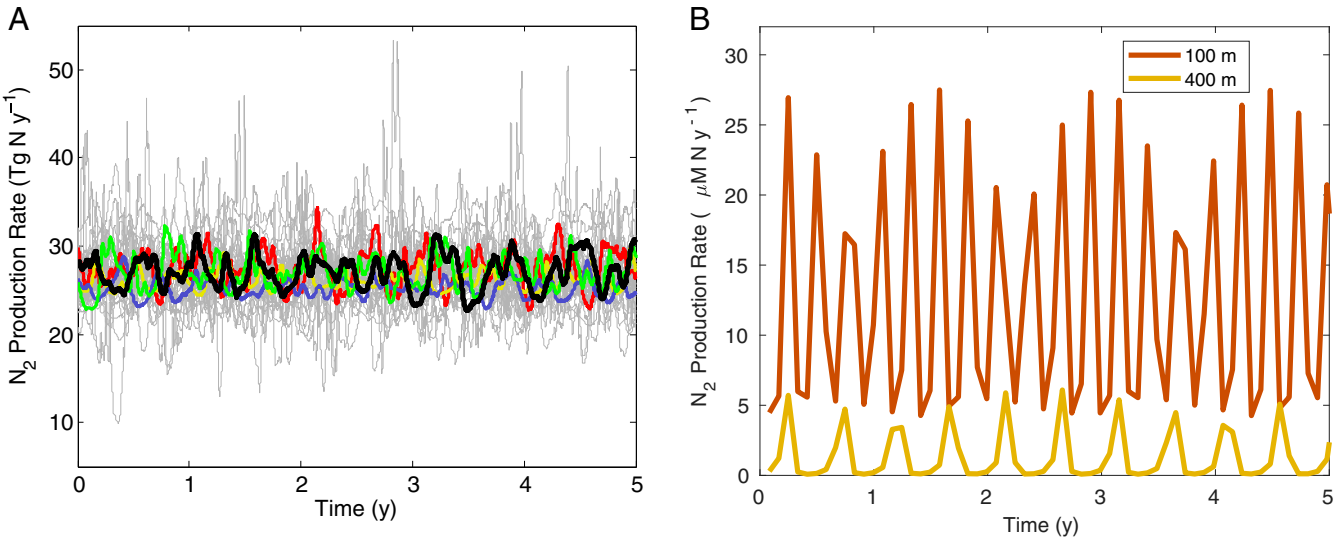

Fig. 1. Time series of unforced variability in the regional and local rates of N loss from the ODZ of the eastern tropical North Pacific. (*A*) Rates (1 Tg N y^{-1} = 10^{12} g N y^{-1}) are spatially integrated across the ETNP in the standard model simulation (black) and sensitivity cases (gray and colors). Fluctuations occur regardless of physiological or ecological uncertainties (*SI Appendix*, Table S1): whether O_2 tolerances of anaerobes are 1 μM (yellow) or ≥10 μM (red), if the two steps of nitrification (NH_4^+ and NO_2^- oxidation) have different nanomolar O_2 sensitivities (green), or if an additional metabolism [dissimilatory nitrate reduction to ammonium (DNRA)] is incorporated into the model (blue). They also hold across wide ranges in other microbial ecosystem parameters (gray, *SI Appendix*, Table S1). (*B*) Time series of local rates of N loss in locations with representative ecosystem oscillations (12°N, 90°W at 100 m and 25°N, 113°W at 400 m).

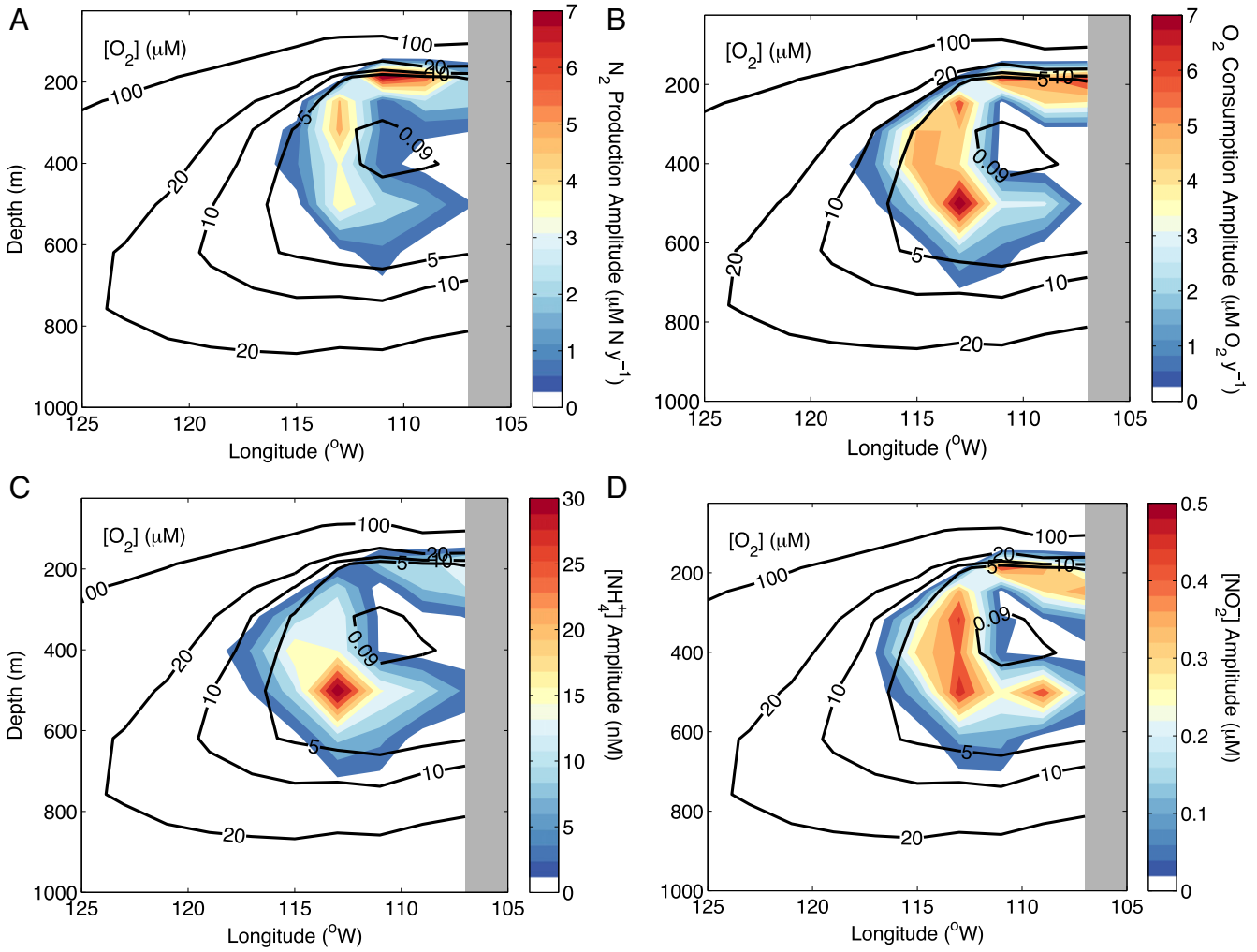

Fig. 2. Spatial distribution of ecologically driven oscillations within the ODZ. The spatial distribution of oscillation amplitudes (colors) is shown along a zonal cross-section through the model ODZ (20–28°N). Oscillation amplitudes are computed as the difference between maximum and minimum values over a 10-y simulation for (*A*) the N loss rate, (*B*) the O_2 consumption rate, and the concentrations of (*C*) NH_4^+ and (*D*) NO_2^-. Variability is overlain by time-mean concentrations of O_2 (in μM; black contours). Gray shading denotes the western coastline of North America.

the available O_2 and NO_2^- (Fig. 3 *A* and *B*, *ii*). The loss of O_2 promotes anaerobic metabolisms, but the loss of NO_2^- also depletes the energy available for heterotrophic growth fueled by denitrification. The NO_2^- oxidizers can short circuit complete heterotrophic denitrification to N_2 because of their higher efficiency of NO_2^- utilization (15), which is required by the model to reproduce the observed distribution of NO_2^- within oxic and anoxic waters (*SI Appendix*, Fig. S6). In contrast, the depletion of NO_2^- has little effect on anammox bacteria because they are generally limited by NH_4^+ in the model, consistent with rate measurements from the ODZs (1, 28). Thus, as NO_2^- is drawn down by oxidation, the decline of heterotrophic denitrification relative to anammox (Fig. 3*C*, *iii*) depletes NH_4^+ to levels that, in turn, limit the NO_2^- oxidizers, slowing their rate of O_2 and NO_2^- utilization (Fig. 3*B*, *iii*). The cessation of O_2 consumption allows its concentration to be gradually replenished by the physical supply, while NO_2^- simultaneously accumulates due to an excess of NO_3^- reduction over NO_2^- oxidation (Fig. 3*A*, *iv*). O_2 accumulation selects against anammox (Fig. 3*C*, *iv*), while NO_2^- accumulation fuels a rapid burst of N loss through heterotrophic denitrification (Fig. 3*D*, *i*). The NH_4^+ liberated from DON during this denitrification pulse restores it to levels that sustain NO_2^- oxidizer growth, a condition that again favors net O_2 consumption, and the oscillation starts anew.

The ecosystem oscillations predicted here arise in a completely steady physical environment, but the supply of organic matter and O_2 to the ODZ exhibit strong temporal variations in the real ocean. We tested the impact of physical variability on the intrinsic ecosystem oscillations by first imposing empirically derived seasonal fluxes of organic particles and then stochastic changes in the rates of ocean circulation (*SI Appendix*, Fig. S7). Ecosystem-driven variability persists, and is even amplified, in the presence of these external forcings, suggesting the oscillations would act as a strong source of variability in the natural environment.

Top-down ecological controls on microbial populations also have the potential to limit fluctuations caused by resource competition. We represented grazing losses in the model by applying a quadratic mortality term to all microbial populations, assuming predation is unselective (*SI Appendix*, Fig. S8). We varied the intrinsic grazing rate by an order of magnitude and find that while the variance in regional N loss is unchanged under weak grazing, under strong grazing the variance is decreased by an order of magnitude (*SI Appendix*, Fig. S8*A*). However, adding this strong grazing term causes an unrealistic build up of NH_4^+ concentration in the anoxic core of the ODZ

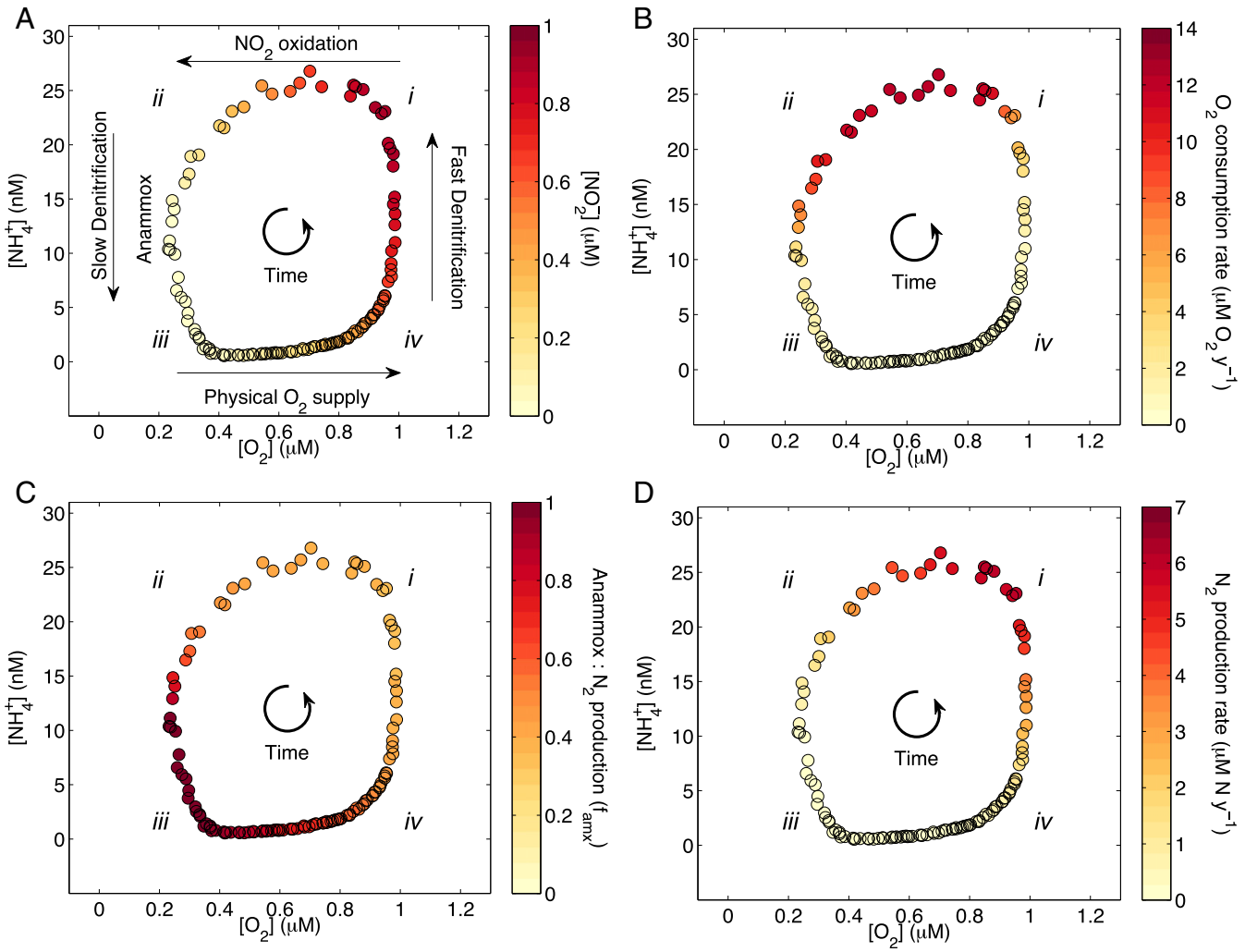

Fig. 3. Dynamics of the ecosystem oscillation. The oscillation of key ecosystem variables is shown in the phase space of NH_4^+ and O_2, from a representative location at the suboxic boundary between the anoxic zone and the oxic ocean (i.e., same as in Fig. 1*B* at 400 m). Time proceeds in the counterclockwise direction, indicated by spiraling arrows. NH_4^+ and O_2 levels are colored by (*A*) the concentration of NO_2^- (μM), (*B*) the rate of O_2 consumption by NO_2^- oxidation (μM O_2 y^{-1}), (*C*) the contribution of anammox to total N_2 production (f_{amx}), and (*D*) the rate of total N_2 production (μM N y^{-1}). Light colors are always either low concentrations or low rates of activity. Straight arrows in *A* identify the dominant process driving changes in NH_4^+ and O_2 during each phase of the cycle. Locations *i*–*iv* marked on the phase diagrams are described in the text.

(*SI Appendix*, Fig. S8*B*). By reducing the biomass of the slow-growing anammox bacteria, grazing lessens the main sink of NH_4^+ in these zones, allowing it to accumulate to persistently high concentrations. The observed distribution of NH_4^+ therefore does not support the grazing rates needed to stabilize the ecosystem oscillations.

The distribution of NH_4^+ within the ODZ provides a unique and detectable geochemical signature of the microbial oscillations (Fig. 4). Over the course of the oscillation, shifts in the balance of NH_4^+ sources and sinks lead to its temporary accumulation within the ODZ, at levels up to ∼10 times the measurable detection limit of the most sensitive technique (∼10–15 nM)—the orthophthalaldehyde (OPA) method. These NH_4^+ spikes are short lived, however, occurring only ∼5% of the time throughout the ODZ (O_2 < 5 μM), such that the average model concentration of NH_4^+ remains below detection. We looked for this potential signature of the oscillation by analyzing 18 depth profiles of NH_4^+ from the ETNP measured using the OPA method (*SI Appendix*, *Supplementary Information Text*). Consistent with the predicted time-mean NH_4^+ concentrations, the average observed concentration of NH_4^+ in waters with O_2 < 5 μM falls below detection. However, in ∼8% of these measurements, we find NH_4^+ concentrations exceeding this detection limit, consistent with the frequency predicted by ecological oscillations. NH_4^+ measurements made with less sensitive conventional techniques suggest spikes are also present in the eastern tropical South Pacific and Arabian Sea ODZs outside the model domain (e.g., refs. 11, 29, and 30), but a quantitative analysis of these features will require more high precision data.

A transient accumulation of NH_4^+ within the ODZ might also be expected from excretion at depth by vertically migrating zooplankton and micronekton (31, 32). Measured NH_4^+ spikes occur up to 100–300 m below the mean depth of diel vertical migration recorded for this region (line and shading in Fig. 4). In contrast, elevated NH_4^+ within the ODZ is found over a similar depth range to where ecological oscillations occur in the model. Temporary spikes of NH_4^+ could also arise from transitory pulses of sinking organic matter that release NH_4^+ into the ODZ faster than it can be consumed. We tested whether changes in the particle flux can produce NH_4^+ spikes, by adding the observed seasonal cycle in net primary production to a model simulation with weak internal oscillations, and thus inherently

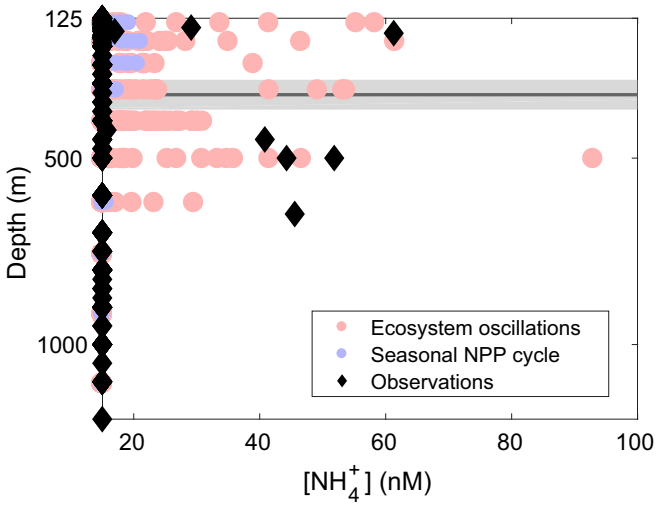

Fig. 4. NH_4^+ depth profiles from the ODZ of the eastern tropical North Pacific in model simulations and observations. Depth profiles were sampled monthly over the course of a year in the standard model simulation (pink circles) and measured on a cruise to the ETNP in 2012 (black diamonds, *SI Appendix, Supplementary Information Text*). NH_4^+ exceeds the detection limit (~15 nM) ~5% of the time in the model simulation and in ~8% of observations at $O_2 < 5$ μM, but on average is below detection in both. Model and observed NH_4^+ values below 15 nM are set to this detection limit. Diel vertical migration depth for the ETNP is plotted (mean indicated by line, SD by shading) (32). The time-dependent NH_4^+ profiles are also shown from a model simulation with a data derived seasonal cycle of net primary production (NPP), but weak internal oscillations (violet). Seasonal fluctuations in the supply of organic matter to the ODZ cannot produce the magnitude of NH_4^+ spikes implied by the observations.

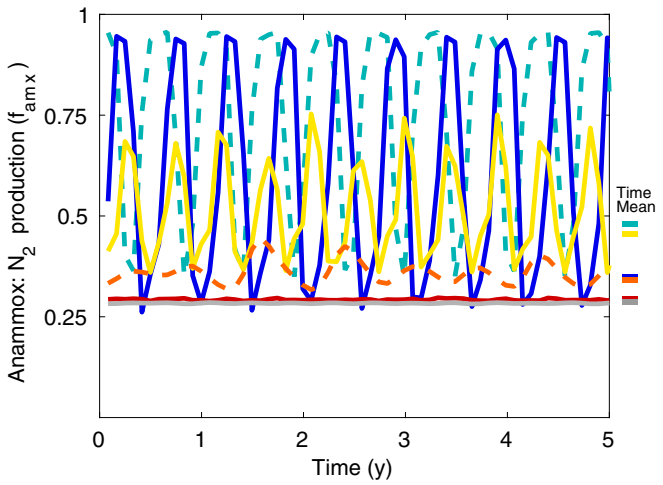

Fig. 5. The contribution of anammox to total N_2 production (f_{amx}) over time. Time series of f_{amx} in representative locations across the ODZ, from 115 m to 450 m. At the oxic–anoxic interface (oxycline), f_{amx} can vary over wide ranges that temporarily obscure its time-mean gradient (blue, cyan, and yellow lines). Within the secondary NO_2^- maximum, f_{amx} approaches the value of 0.28 and oscillations are weak (orange, red, and gray lines). Solid lines are from the heart of the ODZ, whereas dashed lines are from its margins. Time-mean contributions of anammox to N loss are shown as colored horizontal lines on the *Right* axis.

small pulses of NH_4^+. In this case, even with forced fluctuations in the supply of organic matter into the ODZ, the predicted time-varying concentrations of NH_4^+ barely exceed the measured detection limit at any depth. The measured spikes in NH_4^+ therefore support strong nonequilibrium ecosystem behavior.

Ecological oscillations within the ODZ have direct consequences for the fraction of total N loss that derives from anammox (f_{amx}) as opposed to heterotrophic denitrification (Fig. 5). The contribution of these metabolic pathways to N loss has been observed to vary across and within the ODZs from direct rate measurements in the field, but the causes of these variations remain hotly debated (e.g., refs. 2, 4, and 32). During the course of the oscillation, when NO_2^- oxidizing bacteria are ascendant, the NO_2^- that would otherwise be reduced by heterotrophs is reoxidized to NO_3^-. The suppression of heterotrophic denitrification temporarily allows NH_4^+-limited anammox to contribute 100% of local N_2 production. However, after NO_2^- accumulates, the rapid bursts of heterotrophic denitrification vastly exceed previous rates of anammox (Fig. 3 *C* and *D*) and thereby dominate total N loss over a complete oscillatory cycle (horizontal lines Fig. 5). These local variations in the balance of N loss processes can temporarily obscure the time-mean gradients in f_{amx} across the ODZ (15). Because they occur over an extremely narrow range in the concentrations of O_2, NH_4^+, and NO_2^-, evaluating this ecological contribution to observed variations in f_{amx} will require frequent and high-precision measurements of these chemical abundances and associated metabolic rates.

Oscillatory behavior is a common feature of idealized ecosystem models with multiple interacting populations (33, 34), but is rarely shown to persist in realistic representations of the environment such as a three-dimensional ocean circulation. Intrinsic ecosystem oscillations provide a mechanism to generate variations in marine microbial community structure and N and O_2 cycling, which are often ascribed to externally forced changes in physical and chemical conditions. Because these oscillations lack spatial coherence and power at decadal and longer timescales (Fig. 1*A*), they are unlikely to explain large-scale decadal variations in N loss (5). However, dynamics such as these may be pervasive beyond the ODZs, occurring wherever the physical supply of resources selects for a microbial community that over time undermines its own ecological niche by shifting the chemical environment to temporarily favor the growth of its competitors or degrade the growth of its facilitators.

ACKNOWLEDGMENTS. We thank Tim DeVries for supplying the ocean circulation model, H. Frenzel for technical assistance, and C. Fuchsman and A. Santoro for insightful discussions. This work was made possible by grants from the Gordon and Betty Moore Foundation (GBMF 3775 to C.D.) and the Joint Institute for the Study of the Atmosphere and Ocean under NOAA Cooperative Agreement (NA15OAR4320063, contribution no. 2018-0141, to B.X.C.). This work is NOAA-Pacific Marine Environmental Laboratory contribution no. 4772.

1. Lam P, Kuypers MM (2011) Microbial nitrogen cycling processes in oxygen minimum zones. *Annu Rev Mar Sci* 3:317–345.
2. Babbin AR, Keil RG, Devol AH, Ward BB (2014) Organic matter stoichiometry, flux, and oxygen control nitrogen loss in the ocean. *Science* 344:406–408.
3. Deutsch C, Brix H, Ito T, Frenzel H, Thompson L (2011) Climate-forced variability of ocean hypoxia. *Science* 333:336–339.
4. Ward BB, et al. (2009) Denitrification as the dominant nitrogen loss process in the Arabian Sea. *Nature* 461:78–81.
5. Deutsch C, et al. (2014) Oceanography. Centennial changes in North Pacific anoxia linked to tropical trade winds. *Science* 345:665–668.
6. Altabet MA, Francois R, Murray DW, Prell WL (1995) Climate-related variations in denitrification in the Arabian Sea from sediment $^{15}N/^{14}N$ ratios. *Nature* 373:506–509.
7. Brewer PG, Hofmann AF, Peltzer ET, Ussler W, III (2014) Evaluating microbial chemical choices: The ocean chemistry basis for the competition between use of O_2 or NO_3^- as an electron acceptor. *Deep Res Part I* 87:35–42.
8. Dalsgaard T, et al. (2014) Oxygen at nanomolar levels reversibly suppresses process rates and gene expression in anammox and denitrification in the oxygen minimum zone off northern Chile. *MBio* 5:e01966.
9. Zamora LM, et al. (2012) Nitrous oxide dynamics in low oxygen regions of the Pacific: Insights from the MEMENTO database. *Biogeosciences* 9:5007–5022.
10. Kalvelage T, et al. (2011) Oxygen sensitivity of anammox and coupled N-cycle processes in oxygen minimum zones. *PLoS One* 6:e29299.
11. Kalvelage T, et al. (2013) Nitrogen cycling driven by organic matter export in the South Pacific oxygen minimum zone. *Nat Geosci* 6:228–234.

12. Tiano L, et al. (2014) Oxygen distribution and aerobic respiration in the north and south eastern tropical Pacific oxygen minimum zones. *Deep Res Part I* 94:173–183.
13. Bristow LA, et al. (2016) Ammonium and nitrite oxidation at nanomolar oxygen concentrations in oxygen minimum zone waters. *Proc Natl Acad Sci USA* 113: 10601–10606.
14. Bristow LA, et al. (2017) N_2 production rates limited by nitrite availability in the Bay of Bengal oxygen minimum zone. *Nat Geosci* 10:24–29.
15. Penn J, Weber T, Deutsch C (2016) Microbial functional diversity alters the structure and sensitivity of oxygen deficient zones. *Geophys Res Lett* 43:9773–9780.
16. Buchwald C, Santoro AE, Stanley RHR, Casciotti KL (2015) Nitrogen cycling in the secondary nitrite maximum of the eastern tropical North Pacific off Costa Rica. *Global Biogeochem Cycles* 29:2061–2081.
17. Devries T (2014) The oceanic anthropogenic CO_2 sink: Storage, air-sea fluxes, and transports over the industrial era. *Global Biogeochem Cycles* 28:631–647.
18. Penn JL, Weber T, Chang BX, Deutsch D (2019) Data from "Microbial ecosystem dynamics drive fluctuating nitrogen loss in marine anoxic zones." Figshare.com. Available at https://figshare.com/articles/Data_for_Penn_et_al_2019_Microbial_ecosystem_dynamics_drive_fluctuating_nitrogen_loss_in_marine_anoxic_zones_PNAS_/7627439. Deposited March 11, 2019.
19. Devries T, Deutsch C, Primeau F, Chang B, Devol A (2012) Global rates of water-column denitrification derived from nitrogen gas measurements. *Nat Geosci* 5: 547–550.
20. Karstensen J, Stramma L, Visbeck M (2008) Oxygen minimum zones in the eastern tropical Atlantic and Pacific oceans. *Prog Oceanogr* 77:331–350.
21. Antonov JI, et al. (2010) World ocean database 2009. *NOAA Atlas NESDIS 66* (US Government Printing Office, Washington, DC).
22. Fukuda R, Ogawa H, Nagata T, Koike I (1998) Direct determination of carbon and nitrogen contents of natural bacterial assemblages in marine environments. *Appl Environ Microbiol* 64:3352–3358.
23. Fasham MJR, Ducklow HW, McKelvie SM (1990) A nitrogen-based model of plankton dynamics in the oceanic mixed layer. *J Mar Res* 48:591–639.
24. DeVries T, Deutsch C, Rafter PA, Primeau F (2013) Marine denitrification rates determined from a global 3-D inverse model. *Biogeosciences* 10:2481–2496.
25. Lam P, et al. (2009) Revising the nitrogen cycle in the Peruvian oxygen minimum zone. *Proc Natl Acad Sci USA* 106:4752–4757.
26. Tsementzi D, et al. (2016) SAR11 bacteria linked to ocean anoxia and nitrogen loss. *Nature* 536:179–183.
27. Betlach MR, Tiedje JM (1981) Kinetic explanation for accumulation of nitrite, nitric oxide, and nitrous oxide during bacterial denitrification. *Appl Environ Microbiol* 42: 1074–1084.
28. Dalsgaard T, Canfield DE, Petersen J, Thamdrup B, Acuña-González J (2003) N_2 production by the anammox reaction in the anoxic water column of Golfo Dulce, Costa Rica. *Nature* 422:606–608.
29. Widner B, Mordy CW, Mulholland MR (2018) Cyanate distribution and uptake above and within the Eastern Tropical South Pacific oxygen deficient zone. *Limnoly Oceanogr* 63(Suppl 1):S177–S192.
30. Codispoti L (2000) "Temp, salinity, nutrients from Niskin bottles". United States JGOFS Data Server. Woods Hole Oceanographic Institution, USA: U.S. JGOFS Data Management Office'. Available at usjgofs.whoi.edu/jg/serv/jgofs/arabian/ttn-045/bottle.html0%7Bdir=usjgofs.whoi.edu/jg/dir/jgofs/arabian/ttn-045/,info=usjgofs.whoi.edu/jg/info/jgofs/arabian/ttn-045/bottle%7D. Accessed May 8, 2000.
31. Bianchi D, Galbraith ED, Carozza DA, Mislan KAS, Stock CA (2013) Intensification of open-ocean oxygen depletion by vertically migrating animals. *Nat Geosci* 6:545–458.
32. Bianchi D, Babbin AR, Galbraith ED (2014) Enhancement of anammox by the excretion of diel vertical migrators. *Proc Natl Acad Sci USA* 111:15653–15658.
33. Huisman J, Welssing FJ (1999) Biodiversity of plankton by species oscillations and chaos. *Nature* 402:407–410.
34. Huisman J, Pham Thi NN, Karl DM, Sommeijer B (2006) Reduced mixing generates oscillations and chaos in the oceanic deep chlorophyll maximum. *Nature* 439:322–325.